

**This is a self-archived version of an original article. This version may differ from the original in pagination and typographic details.**

**Author(s):** Mannisto, Jere K.; Pavlovic, Ljiljana; Heikkinen, Johannes; Tiainen, Tony; Sahari, Aleks; Maier, Norbert M.; Rissanen, Kari; Nieger, Martin; Hopmann, Kathrin H.; Repo, Timo

**Title:** N-Heteroaryl Carbamates from Carbon Dioxide via Chemoselective Superbase Catalysis : Substrate Scope and Mechanistic Investigation

**Year:** 2023

**Version:** Published version

**Copyright:** © The Authors. Published by American Chemical Society

**Rights:** CC BY 4.0

**Rights url:** <https://creativecommons.org/licenses/by/4.0/>

**Please cite the original version:**

Mannisto, J. K., Pavlovic, L., Heikkinen, J., Tiainen, T., Sahari, A., Maier, N. M., Rissanen, K., Nieger, M., Hopmann, K. H., & Repo, T. (2023). N-Heteroaryl Carbamates from Carbon Dioxide via Chemoselective Superbase Catalysis : Substrate Scope and Mechanistic Investigation. *ACS Catalysis*, 13, 11509-11521. <https://doi.org/10.1021/acscatal.3c02362>

# N-Heteroaryl Carbamates from Carbon Dioxide via Chemoselective Superbase Catalysis: Substrate Scope and Mechanistic Investigation

Jere K. Mannisto, Ljiljana Pavlovic, Johannes Heikkinen, Tony Tiainen, Aleksu Sahari, Norbert M. Maier, Kari Rissanen, Martin Nieger, Kathrin H. Hopmann,\* and Timo Repo\*



Cite This: *ACS Catal.* 2023, 13, 11509–11521



Read Online

ACCESS |

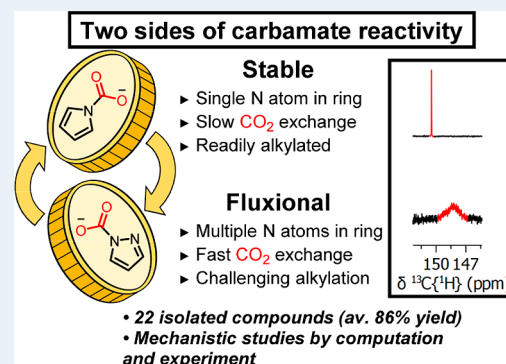
Metrics & More

Article Recommendations

Supporting Information

**ABSTRACT:** We report a mild superbase-catalyzed and nitrogen-selective carboxylation of *N*-heteroaryls, with subsequent alkylation enabling the synthesis of drug-like *O*-alkyl carbamates in good yields (av. 86%). Our findings suggest a partial revision of the current mechanistic understanding as superbases upon mixing with indoles and azoles generally form uncharged hydrogen-bonded complexes and not ionic salts as previously proposed. However, when these complexes are exposed to CO<sub>2</sub>, carbamate salts are formed. These can be categorized into two subgroups, stable and fluxional carbamate salts, where the latter undergo fast and reversible CO<sub>2</sub> exchange, thus being poor substrates for alkylation. Experiments and DFT calculations indicate that the fluxional behavior is primarily caused by substrate-specific electronic destabilization effects. The degree of destabilization depends on the number of nitrogen atoms within and the functional group substitution on the heterocyclic ring structures. Fluxionality can be compensated for by the use of lower temperatures and/or higher CO<sub>2</sub> pressures as both measures stabilize the carbamate salts sufficiently, enabling subsequent alkylation.

**KEYWORDS:** carbon dioxide, heterocycles, superbases, carboxylation, mechanisms, computations, NMR



## INTRODUCTION

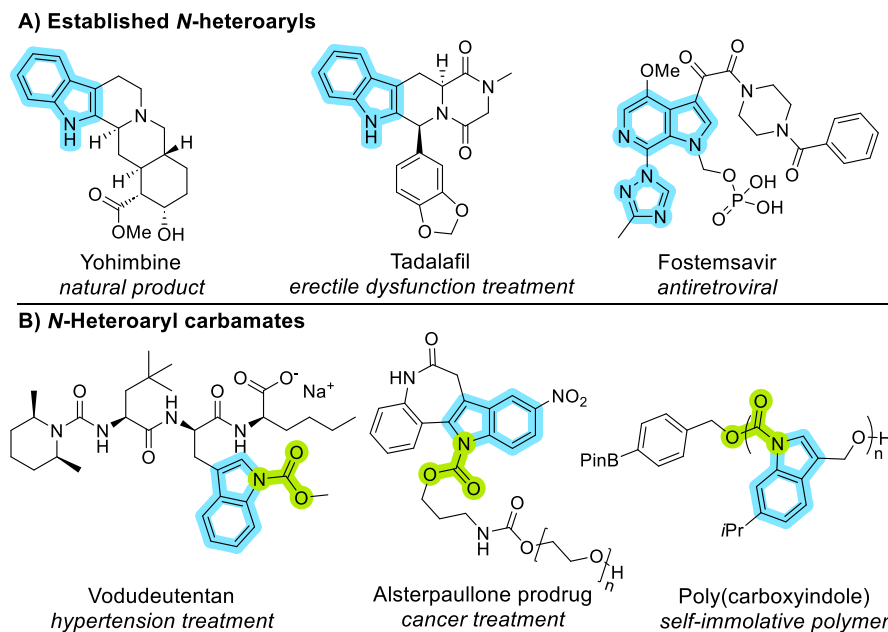
Nitrogen-containing heteroaryls, such as indoles and azoles, are important constituents of natural products and many FDA-approved small-molecule pharmaceuticals (Scheme 1A).<sup>1–3</sup> Consequently, there have been extensive research efforts on *N*-heteroaryl functionalization and derivatization, which are essential for the development of new chemical compounds for medicinal and other applications.<sup>4–9</sup> Carboxylation at the nitrogen position leads to the formation of carbamates which are prodrug elements and key motifs in many pharmaceuticals.<sup>10–13</sup> Indeed, *N*-heteroaryl carbamates are promising medicinal targets due to their potential in improving physiochemical properties and stabilities under biological conditions (Scheme 1B).<sup>13,14</sup> A recent example involves the utilization of *N*-heteroaryl carbamates as intermediates in the prodrug development of pibrentasvir.<sup>15</sup> Carbamates based on *N*-heteroaryls have also been applied as degradable polymers.<sup>16</sup>

Carbon dioxide (CO<sub>2</sub>) is a synthetically attractive molecule as it is a non-toxic, inexpensive, and readily available C1-source.<sup>12,17</sup> The use of CO<sub>2</sub> has received significant attention in the functionalization of *N*-heteroaryls, particularly in C–C bond formation.<sup>5–7</sup> The alternative C–N bond formation, resulting in the formation of carbamates, is well-known for saturated *N*-heterocycles (Scheme 2A).<sup>11,17</sup> However, carbamate formation using CO<sub>2</sub> and *unsaturated N*-heterocycles (*N*-heteroaryls) is a much less explored field (Scheme 2B).

Indoles, an important subgroup of *N*-heteroaryls, can be *N*-carboxylated using *n*-BuLi; however, the use of a hard base severely limits functional group compatibility.<sup>18–21</sup> Additionally, the inherent nucleophilic reactivity of indoles resides at the C3 position,<sup>22</sup> implying that most CO<sub>2</sub>-based carboxylations take place here.<sup>5,23–25</sup> Consequently, directing reactivity to nitrogen N1 is challenging.<sup>26,27</sup> A recent report detailed indole *N*-carboxylation as part of an intramolecular cyclization.<sup>28</sup> The current state-of-the-art approach to accessing indole *O*-alkyl carbamates involves a two-pot process (Scheme 2C).<sup>29,30</sup> Alcohols are transformed to imidazole carbamates, and once isolated, these can be used to transfer the carbamate moiety to indoles. It would be advantageous if the desired indole *O*-alkyl carbamates could be prepared directly from benign CO<sub>2</sub> without the need to prepare and isolate imidazole carbamates. For related azole-based substrates, *N*-formylated products can be obtained with CO<sub>2</sub> under reductive conditions, whereas carbamates can be formed catalytically using an NHC–copper complex.<sup>31–33</sup>

Received: May 25, 2023

Revised: July 25, 2023

Scheme 1. Selected Examples of Important *N*-Heteroaryls (A) and Corresponding Carbamates (B)

Selective formation of desired products from *N*-heteroaryls requires a good understanding of their inherent reactivities. *N*-Heteroaryls have found widespread application in ionic liquids as the anionic component (Scheme 2D).<sup>34–48</sup> The cationic component can be a tetraalkylphosphonium,<sup>36–39</sup> an azolium (HetAr<sup>+</sup>),<sup>40,41</sup> or a superbases, such as TMG, DBU, or MTBD, which are proposed to deprotonate *N*-heteroaryls.<sup>42–48</sup> The resulting salts interact with CO<sub>2</sub>, but the mechanistic details are not thoroughly understood.<sup>49,50</sup> The behavior of ionic liquids is important to understand for rationalizing their role as modulators and enhancers of heterogeneous catalysts.<sup>51–53</sup> Superbases have many important applications as catalysts and stoichiometric reagents.<sup>54</sup> Consequently, understanding superbases-mediated nucleophile activation is critical for designing new reactions.<sup>55</sup> We reasoned that the superbases-mediated activation of *N*-heterocycles could enable a convenient and complementary CO<sub>2</sub>-based entry to the synthesis of *N*-heteroaryl carbamates. Herein, we present a one-pot method toward in situ conversion of *N*-heteroaryls and CO<sub>2</sub> to carbamate anions, followed by a facile reaction with available alkyl bromides (Scheme 2E). Using this approach, structurally diverse indole carbamates are obtained with complete selectivity for nitrogen N1 in high yields and under mild conditions. Our mechanistic analysis reveals clear trends in the reactivity of *N*-heteroaryls with CO<sub>2</sub>, leading to a partial revision of the currently accepted mechanistic understanding.

## RESULTS AND DISCUSSION

**Indole Carboxylations and Reaction Scope.** Initially, we investigated the reactivity of unsubstituted indole **1a** with 1-bromopentane under 1 bar CO<sub>2</sub> (Scheme 3). After optimization (Supporting Information, Section S11), we found that the reaction could be conducted under stoichiometric conditions (condition A) or alternatively under catalytic conditions (condition B). The latter produced *O*-alkyl carbamate **2a** in a superior yield. Carboxylation occurred exclusively at N1, *i.e.*, no reaction at C3 was observed.

The generality of the reaction was explored for electronically varied indoles. Electron-donating (**2b** and **2c**) and moderately

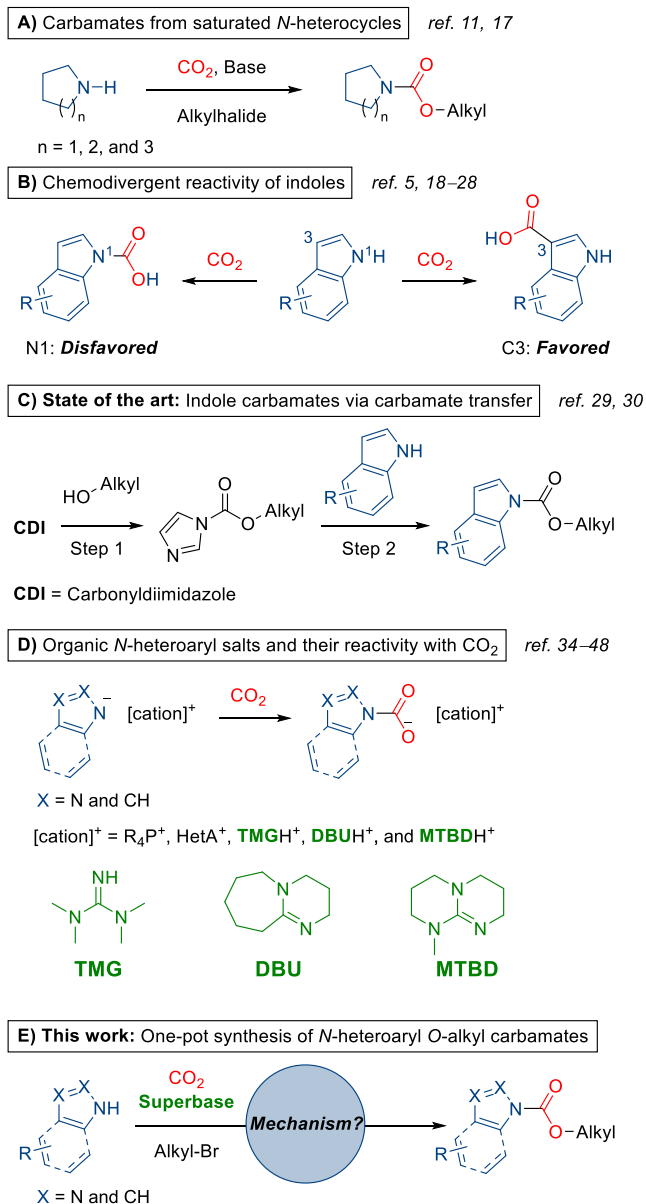
electron-withdrawing substituents (**2d–g**) are well tolerated. Strongly electron-deficient *O*-alkyl carbamates **2h** and **2i** can be formed *via* conditions A and B but with significant quantities of *N*-alkylated byproduct **3** (Supporting Information, Section S11.3). Gratifyingly, increasing the CO<sub>2</sub> pressure to 40 bar and using 1-iodopentane (Scheme 3, condition C) suppressed the formation of byproduct **3**, thereby providing the desired *O*-alkyl carbamates in good yields.

The structural variation of the indole ring system was explored next. Introduction of a second nitrogen atom (azaindole **2j**) is only compatible with condition A, while adding a fused benzene ring (**2k**) or removing one (**2l**) is well tolerated. More complex substrates such as the sleep hormone melatonin (**2m**) and biologically relevant tryptophan derivatives (**2n** and **2o**) are well tolerated, with enantiopurity preserved under catalytic condition B. Curiously, indoles bearing substituents adjacent to the nitrogen center fail to react with CO<sub>2</sub> (**1p** and **1q**). These indoles are also known to be unreactive in carbamate transfer (Scheme 2C).<sup>29</sup>

The scope of alkyl bromides utilizing condition B was then explored (Scheme 4). Complex functionalities are well tolerated, including heterocycles and secondary bromides. Drug-like compounds **4a–f** and **4r–g** are prepared in a facile manner. The structure of **4a–e** was confirmed by X-ray crystallography.<sup>56</sup>

We conclude that the developed conditions A, B, and C provide facile access to indole *O*-alkyl carbamates **2** and **4**, with sensitive synthetic handles such as aldehyde (**2f**), boronic ester (**2g**), Weinreb amide (**2n**), and alkyne (**4a**) remaining intact. In the absence of CO<sub>2</sub>, only the *N*-alkylated byproduct **3** is observed (Supporting Information, Section S11). The superbases is a critical component as its absence dramatically decreases the carbamate yield, leading to the formation of significant quantities of **3**. To understand the role of the superbases, we turned toward exploring the reaction mechanism.

**Mechanistic Studies on Indole Carboxylations.** On the basis of literature results and our previous work, we propose a catalytic reaction pathway for superbases-mediated carboxyla-

Scheme 2. Reactivity of *N*-Heterocycles with CO<sub>2</sub>

tion of indoles (Scheme 5).<sup>57,58</sup> Initially, the superbase reacts with CO<sub>2</sub> and indole **1a**, forming a *mixed carbamate*. The latter reacts with the alkyl bromide through an S<sub>N</sub>2-type reaction, forming the observed product **2a**. The superbase is regenerated by Cs<sub>2</sub>CO<sub>3</sub>. In the absence of a superbase, Cs<sub>2</sub>CO<sub>3</sub> can mediate the reaction; however, cesium carbamate salt **5a** seems to be significantly more unstable than the superbase-derived mixed carbamate. We deduce this from the substantially lowered yields of product **2a** and the large quantities of byproduct **3a**. DFT calculations (PBE0-D3BJ[IEFPCM(DMF)]) on the reaction of **1a** with CO<sub>2</sub> in the presence of the superbase TMG show that the proposed mixed carbamate formation has a feasible barrier of 16.1 kcal/mol (313 K, Supporting Information, Section S1.2). In contrast, the competing *N*-alkylation has a high barrier of 33.0 kcal/mol, in line with the experimentally observed absence of byproduct **3a**.

The key step of mixed carbamate formation was investigated in situ NMR (Scheme 6A). We employed TMG as the

base as it produces simpler NMR spectra than DBU while being catalytically comparable (Supporting Information, Section S11.1). Reference spectra were first measured of indole **1a** and TMG under argon (Scheme 6A). Under these conditions, TMG and indole **1a** appear to form a hydrogen-bonded complex as indole **1a** NH is shifted downfield by 0.11 ppm by <sup>1</sup>H NMR in the presence of TMG. Similar bonding is known for anilines.<sup>58</sup> The complex appears to consist of neutral components, as judged from the TMG central carbon <sup>13</sup>C{<sup>1</sup>H} resonance at 166.3 ppm, which is close to freebase at 166.2 ppm.<sup>58</sup> This finding seems to contradict previous literature, which has proposed that indole **1a** is deprotonated by superbases.<sup>43</sup> However, DFT calculations (PBE0-D3BJ-IEFPCM(DMF)), Supporting Information, Section S1.3) support our experimental findings, predicting a cost of 5 to 8 kcal/mol for forming ionic salts from TMG and indoles **1a**, **1h**, or **1q**. Known pK<sub>a</sub> values for indole **1a** (21.0) and TMG (13.2) in DMSO also support that the indole **1a**–TMG complex remains fully neutral (Supporting Information, Section S4.1).<sup>59–61</sup>

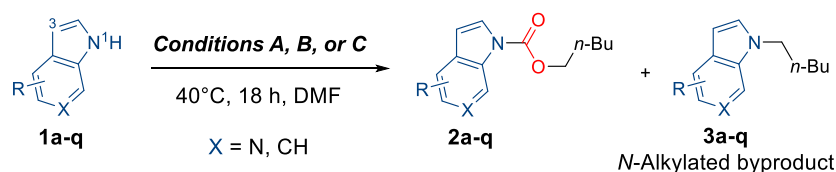
We proceeded to measure the NMR of indole **1a** and TMG under CO<sub>2</sub> (1 bar). Under these conditions, TMG becomes protonated as the central carbon is now observed at 162.0 ppm (Scheme 6A). This is consistent with the formation of a mixed carbamate, which is also supported by the appearance of the indole carboxylate as a new <sup>13</sup>C{<sup>1</sup>H} resonance at 151.8 ppm. It was further assessed if the change from a neutral complex (under argon) to an ionic salt (under CO<sub>2</sub>) can be observed with other NMR-active nuclei. The difference between freebase and protonated TMG is *ca.* 0.3 ppm by <sup>1</sup>H NMR. While this is a meaningful difference, we felt a larger absolute value would be beneficial in determining the protonation state of TMG. In this regard, we found that <sup>15</sup>N NMR at natural isotopic abundance is very sensitive since the difference between freebase and protonated TMG is up to 80 ppm (Supporting Information, Section S4.4). The <sup>15</sup>N NMR results clearly indicate that the indole **1a**–TMG complex is neutral under argon but forms an ionic mixed carbamate under CO<sub>2</sub>.

While <sup>15</sup>N NMR is accurate, we recognize the long acquisition times (15–48 h). As a compromise between high sensitivity and short acquisition times, we advocate the use of <sup>13</sup>C{<sup>1</sup>H} NMR in studying whether *N*-heteroaryl–superbase complexes are neutral or ionic. This strategy is based on the key observation that the signal from the central carbon of TMG is sensitive to protonation. Under our conditions, good-quality spectra (of TMG) are obtained in 1 min. The total change in the chemical shift of the TMG central carbon, Δδ(<sup>13</sup>C), is provided in Scheme 6 using eq 1. This equation assesses changes in protonation state when changing the atmosphere from argon to CO<sub>2</sub>. For example, if a *N*-heteroaryl–TMG complex is a fully ionic salt under argon, then switching to CO<sub>2</sub> should not affect the protonation state of TMG, resulting in Δδ(<sup>13</sup>C) = 0. The generality of eq 1 was also demonstrated for other complexes of *N*-heteroaryls and superbases (*vide infra*).

$$\Delta\delta(^{13}\text{C}) = \delta(^{13}\text{C}[\text{CO}_2]) - \delta(^{13}\text{C}[\text{Ar}]) \quad (1)$$

We continued by studying a selection of 5-substituted indoles in order of increasing electron-deficiency by the Hammett constant σ<sub>p</sub> (Scheme 6B). NMR spectra were recorded first under argon and then under CO<sub>2</sub> (1 bar). In all cases, there was a large change in the protonation state of

## Scheme 3. Indole Carboxylation Scope

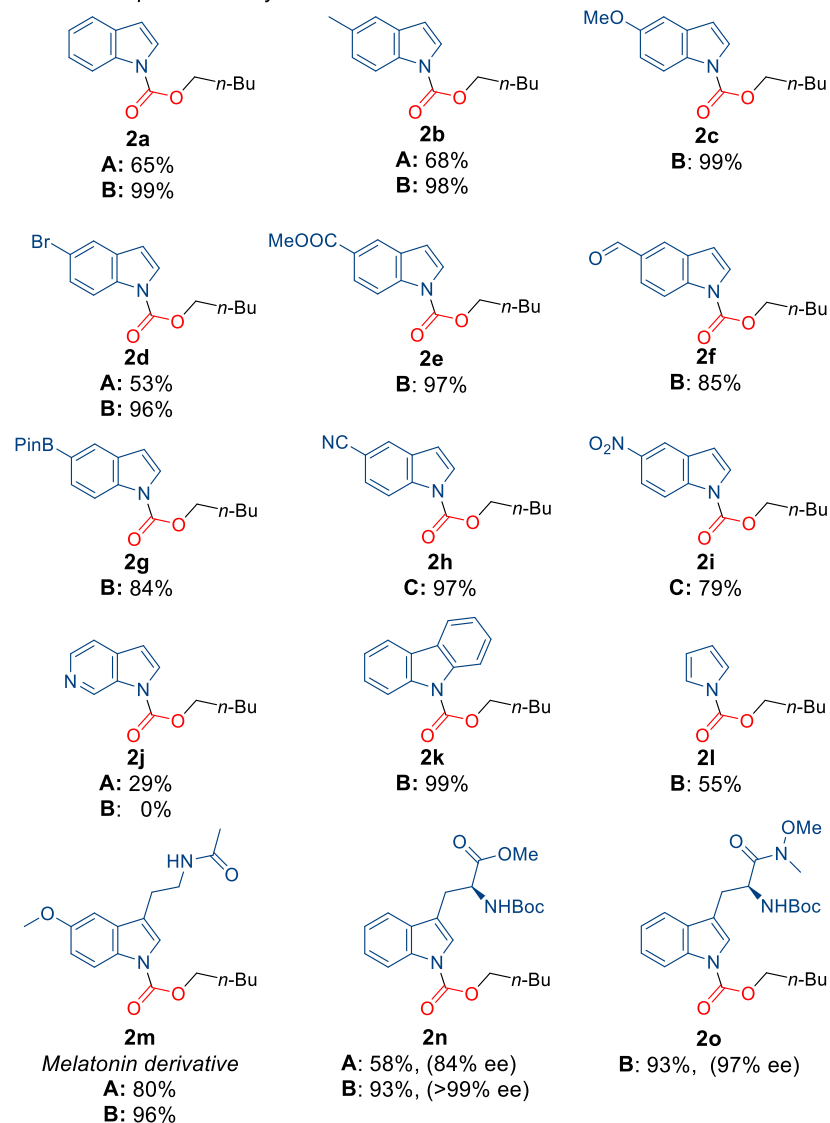


**A:** DBU (2 equiv), 1-Bromopentane (2 equiv), and CO<sub>2</sub> (1 bar)

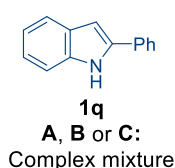
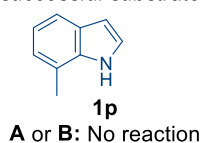
**B:** DBU (20 mol%), Cs<sub>2</sub>CO<sub>3</sub> (4 equiv), 1-Bromopentane (2 equiv), and CO<sub>2</sub> (1 bar)

**C:** As condition B, but 1-Iodopentane (3 equiv.) and CO<sub>2</sub> (40 bar)

Reaction scope - isolated yields:



Unsuccessful substrates

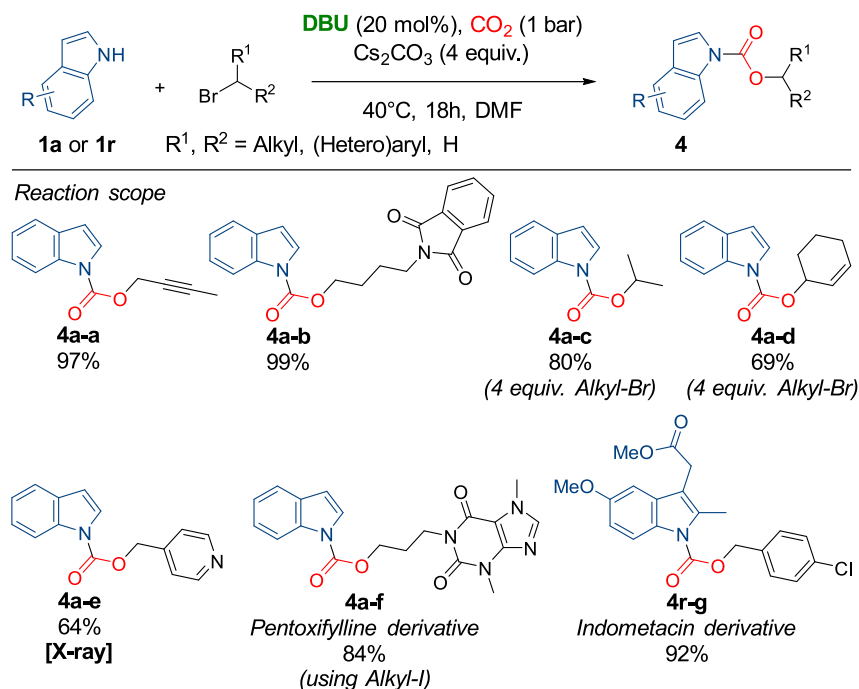


TMG ( $\Delta\delta(^{13}C) \approx -4$  ppm). This indicates that the studied indole-TMG complexes are neutral under argon but form

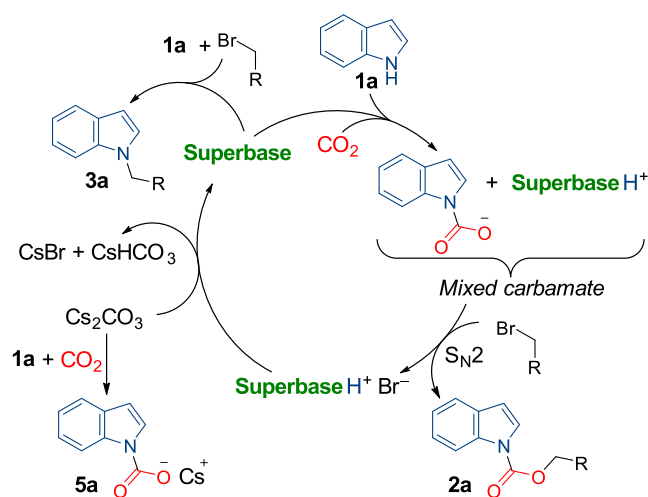
ionic salts under CO<sub>2</sub>. The electronics of the parent indoles have a significant effect on the carboxylation behavior of the



## Scheme 4. Alkyl Bromide Scope in Catalytic Indole Carboxylation (Condition B)



## Scheme 5. Proposed Catalytic Cycle for the Formation of Indole-Derived O-Alkyl Carbamates

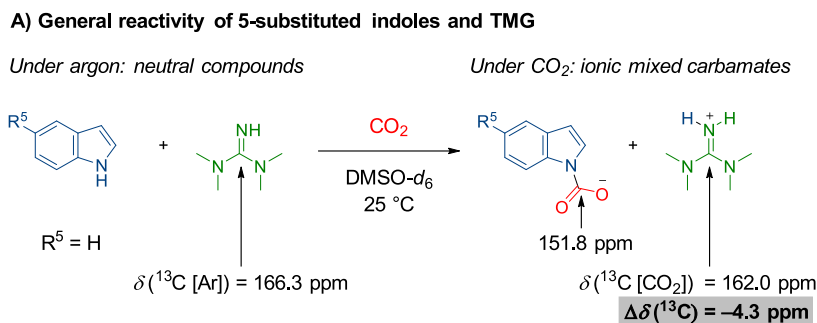
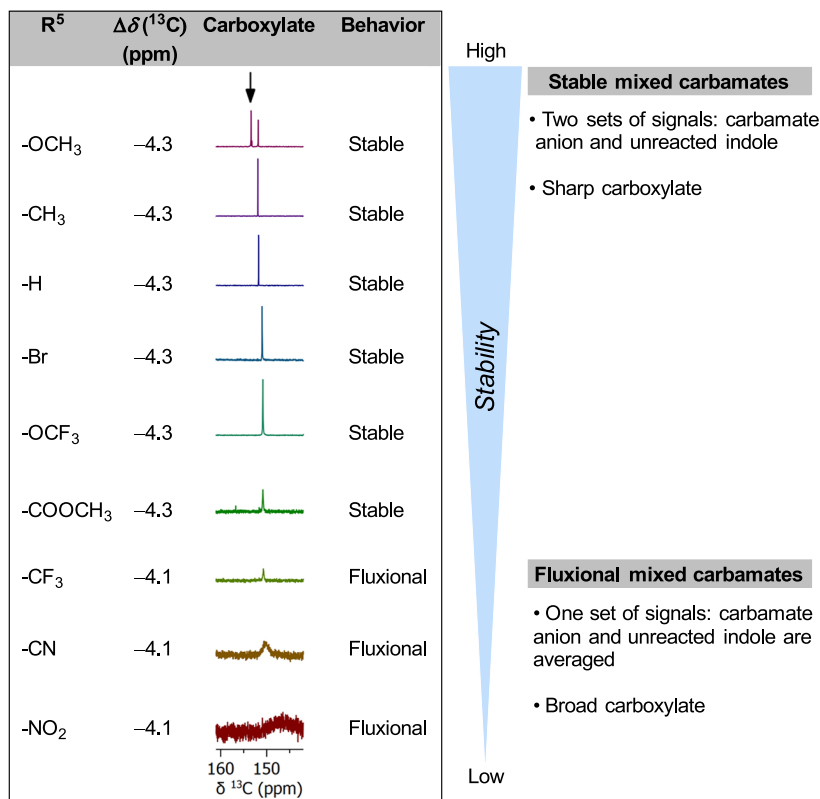


resulting mixed carbamates. The three most electron-rich indoles in the series (5-OMe, -Me, and -H) display well-separated signals of unreacted indole and product (carbamate anion) by <sup>1</sup>H and <sup>13</sup>C{<sup>1</sup>H} NMR, allowing determination of the in situ yield (83, 82, and 80%, respectively). The corresponding carboxylate <sup>13</sup>C{<sup>1</sup>H} signal (151.8–153.4 ppm) is sharp and of high intensity (Scheme 6B), similar to the carboxylate signal of aniline-derived carbamates.<sup>58</sup> This implies that these particular indole-derived mixed carbamates are quite stable on the NMR time scale due to slow CO<sub>2</sub> exchange. However, for more electron-deficient indoles, there is a trend of gradually increasing fluxionality (decreased stability), as is exemplified by the incremental broadening of the carboxylate <sup>13</sup>C{<sup>1</sup>H} resonance (Scheme 6B). For the three most electron-deficient indoles (5-CF<sub>3</sub>, -CN, and -NO<sub>2</sub>), unreacted indole is not observable under CO<sub>2</sub> (1 bar). Instead, the starting material and product (carbamate anion) are

observed as a single set of broad and low-intensity signals due to rapid CO<sub>2</sub> exchange on the NMR time scale.<sup>58</sup> A rapid CO<sub>2</sub> exchange rate is supported by the fact that these indoles require elevated CO<sub>2</sub> pressure (40 bar) to suppress the formation of *N*-alkylated byproduct 3 (Scheme 3 and Supporting Information, Section S11.3). The higher CO<sub>2</sub> pressures likely stabilize the fluxional behavior and, therefore, the mixed carbamate has a sufficient life time to react with alkyl bromides.

If fluxional behavior was to be caused by rapid CO<sub>2</sub> exchange, the equilibrium would also be expected to be sensitive to thermal effects.<sup>58</sup> In this regard, we performed variable-temperature NMR studies (VT-NMR) in DMF-*d*<sub>7</sub>, similar in properties to DMSO-*d*<sub>6</sub> but melting at lower temperatures. Electron-deficient and highly fluxional 5-cyanoindole 1h was chosen as the substrate (Figure 1). Once CO<sub>2</sub> (1 bar) is applied, the resonances of protons H7 and H2 become very broad. In the carbon spectrum, there is significant line broadening, particularly for carbons adjacent to N1. This is accompanied by N1 no longer being detectable by <sup>15</sup>N NMR. Lowering the temperature to -25 °C stabilizes the mixed carbamate, as is evident from the increased sharpness and intensity of H7 and H2, as well as the overall sharpening of the <sup>13</sup>C{<sup>1</sup>H} spectrum. Moreover, N1 is again detectable by <sup>15</sup>N NMR. In other words, when the rate of CO<sub>2</sub> exchange is fast, the reactive nitrogen atom is not detectable by <sup>15</sup>N NMR. The NMR behavior of 5-cyanoindole 1h indicates that low temperatures can stabilize fluxional mixed carbamates by reducing the rate of CO<sub>2</sub> exchange. Finally, the effect of pressure was evaluated by in situ NMR at 25 °C (Supporting Information, Section S14.3). Increasing pressure from 1 bar CO<sub>2</sub> to 5 bar has no observable effect on 5-cyanoindole 1h by <sup>1</sup>H or <sup>13</sup>C{<sup>1</sup>H} NMR. However, a slight increase in stabilization is observed at 10 bar CO<sub>2</sub> by <sup>1</sup>H NMR. These changes are of lesser magnitude in comparison to thermal stabilization, *i.e.*, when the sample is cooled from 25 to 0 °C.

## Scheme 6. NMR Assessment of 5-Substituted Indoles with TMG (1 equiv)

**B) The influence of electronic effects on 5-substituted indoles**

Detailed insights into the operative carboxylation pathways were obtained from computational modeling of different indoles (PBE0-D3BJ[IEFPCM(DMF)]<sub>298 K</sub>). Our analysis shows that TMG pre-associates to the indole through hydrogen bonding. The subsequent attack on CO<sub>2</sub> occurs concertedly with proton transfer from indole **1a** to TMG (Figure 2).<sup>58</sup> The computed Gibbs free energies at 298 K show a favorable barrier of 15.7 kcal/mol for this step, with a reaction energy of -2.8 kcal/mol (Table 1, entry 1), in line with the experimentally observed reactivity. Electron-deficient 5-cyanoindole **1h** also provides a favorable computed barrier and reaction energy (entry 2). Interestingly, indoles **1p** and **1q**, which failed to produce any carbamate in our experiments (Scheme 3), display feasible barriers but endergonic reaction energies (2.6 and 4.0 kcal/mol), indicating that decarboxylation is faster than carboxylation (Table 1, entries 3–4). The optimized geometries of products **1a** and **1h** show that the carboxylate is nearly in-plane ( $\theta \approx 15^\circ$ , entries 1–2). In contrast, in the products of **1p** and **1q**, the adjacent methyl and phenyl substituents force the carboxylate out-of-plane ( $\theta \approx$

$40^\circ$ , entries 3–4), reducing non-covalent charge stabilization compared to **1a** and **1h** (see Supporting Information, Section S1.4).

**Differing Reactivity of Azoles.** Having successfully reacted CO<sub>2</sub> with indoles and pyrrole, we proceeded to investigate structurally related azoles **1s–w** (Scheme 7). Generally, complex product mixtures or *N*-alkylated by-products **3** were obtained, which gave us the initial impression that azoles do not react with CO<sub>2</sub>. We turned our attention toward understanding this apparent lack of reactivity from a mechanistic perspective.

First, we pondered if the interaction between azoles and superbases differs from that between indoles. Previous literature has proposed that azoles and indoles are deprotonated by superbases, forming ionic liquids.<sup>42–48</sup> However, our computational studies show that azole–TMG complexes, just as indole–TMG complexes, prefer to be neutral, with the exception of tetrazole–TMG and 4-nitroimidazole–TMG (Supporting Information, Section S1.3). Additionally, the predicted extent of salt formation was estimated based on

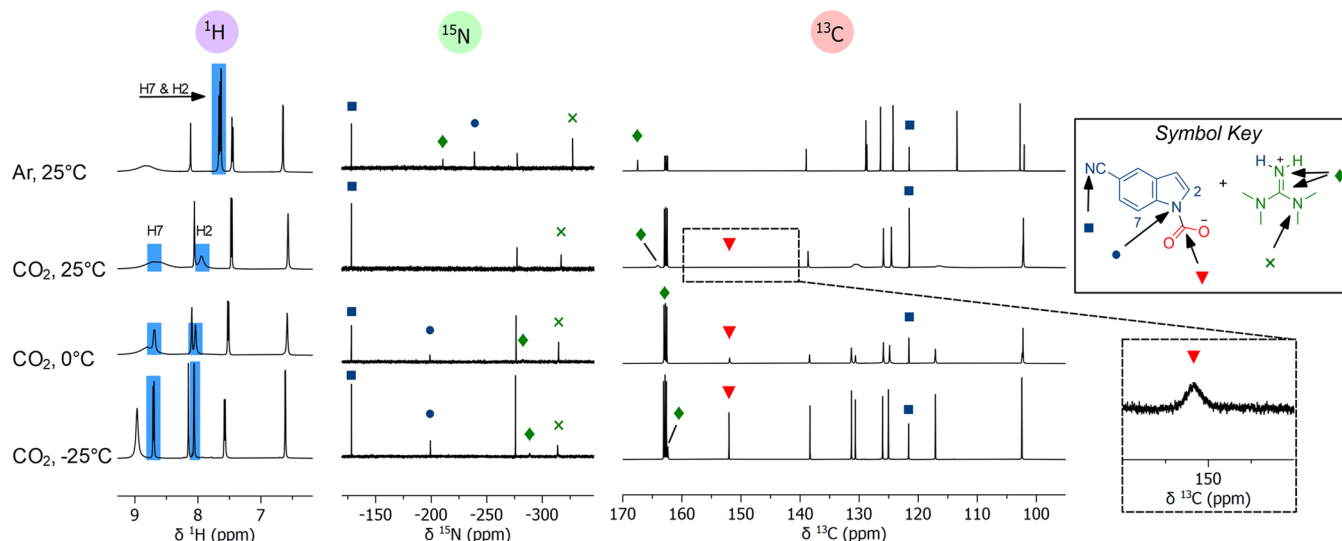


**Figure 1.** VT-NMR spectra (selected regions) of 5-cyanoindole **1h** and TMG (1 equiv) in DMF- $d_7$ . For complete spectra, see [Supporting Information](#), Section S9.1.

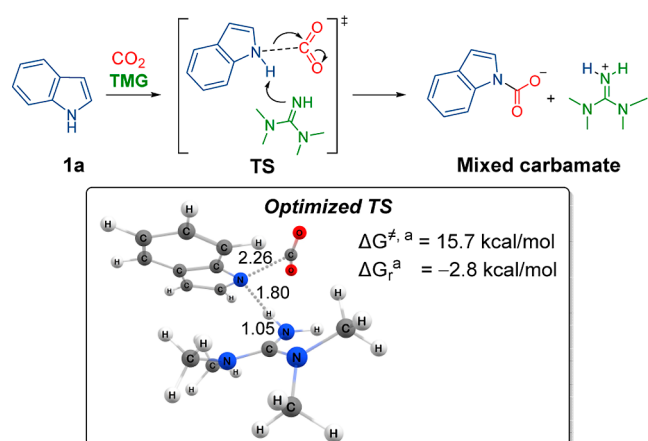


**Figure 2.** Mechanism for indole carboxylation and optimized TS for indole **1a**.  $^a\Delta G_{1M}^\ddagger$ , 298 K, PBE0-D3BJ[IEFPCM(DMF)], and distances are in Angstrom.

**Table 1.** Computed Free Energies for Mixed Carbamate Formation of Indoles with TMG

$$1 + \text{TMG} \xrightarrow{\text{CO}_2} \text{TMGH}^+ + \text{Mixed Carbamate}$$

entry	compound	substitution <sup>a</sup>	$\Delta G^{\ddagger,b}$	$\Delta G_r^b$	$\Theta$ (deg) <sup>c</sup>
1	<b>1a</b>		15.7	-2.8	13.1
2	<b>1h</b>	R <sup>5</sup> = CN	14.1	-2.2	14.5
3	<b>1p</b>	R <sup>7</sup> = CH <sub>3</sub>	17.0	2.6	42.0
4	<b>1q</b>	R <sup>2</sup> = Ph	16.0	4.0	35.0

<sup>a</sup>Unless specified otherwise, R<sup>2</sup>, R<sup>5</sup>, and R<sup>7</sup> = H. <sup>b</sup> $\Delta G_{1M}^\ddagger$ , kcal/mol, 298 K, PBE0-D3BJ[IEFPCM(DMF)]. <sup>c</sup>Dihedral angle defined by C2-N1-C-O1.

known  $pK_a$  values, and the results were aligned with the computed energies ([Supporting Information](#), Section S4.3).<sup>59–61</sup>

Our DFT-based analysis of the carboxylation reactions indicates that pyrrole **1l** has a favorable barrier and reaction energy ([Table 2](#), entry 1), being similar in value to those

indoles that yield isolable *O*-alkyl carbamates ([Table 1](#), entries 1 and 2). This is in line with the experimentally obtained product **2l** ([Scheme 3](#)). Azoles **1s–w** contain multiple nitrogen atoms in the ring structure, assigned as pyridine-like or pyrrole-like ([Table 2](#) graphic). For both nitrogen types, all azoles show feasible carboxylation barriers; however, there is a clear preference for the pyridine-like nitrogen atom. An exception is **1w**, likely due to the proximity of the nitro-group. The computed reaction energy of pyrazole **1s** (entry 2) is favorable toward the formation of carbamate, although slightly less when compared to pyrrole **1l**, whereas the other azoles (**1t**, **1u**, **1v**, and **1w**, entries 3–6) display endergonic reaction energies. The lack of isolable products in experiments ([Scheme 7](#)) can be explained by the endergonic reaction energies, which imply that the reverse decarboxylation barriers are lower than the carboxylation barriers.

To obtain additional experimental support for our hypothesis of fast carboxylation-decarboxylation, we performed in situ NMR studies. Pyrrole **1l** ( $pK_a$  23.0), which forms a neutral complex with TMG ( $pK_a$  13.2) under argon ([Scheme 8A](#)), becomes ionic when CO<sub>2</sub> (1 bar) is applied ( $\Delta\delta(^{13}\text{C}) = -4.0$  ppm).<sup>60</sup> The mixed carbamate forms in 80% yield by <sup>1</sup>H NMR, while the carboxylate  $\delta(^{13}\text{C})$  signal at 150.5 ppm is sharp and of high intensity ([Figure 3](#)), indicating that pyrrole forms a stable mixed carbamate.

Pyrazole **1s** ( $pK_a$  19.8), which contains two nitrogen atoms in the ring ([Scheme 8B](#)), forms a neutral complex under argon.<sup>60</sup> When CO<sub>2</sub> (1 bar) is applied, TMG becomes protonated ( $\Delta\delta(^{13}\text{C}) = -3.2$  ppm). This suggests that a mixed carbamate has formed, yet no carboxylate was initially observed. Performing a longer <sup>13</sup>C{<sup>1</sup>H} NMR experiment revealed broad signals ([Figure 4](#)), which we assign to pyrazole carboxylate (148.2 ppm), the ring of carboxylated pyrazole (138.2 and 129.3 ppm), and unreacted pyrazole (132.9 ppm). The broad, low-intensity signals are indicative of fluxionality, *i.e.*, rapid carboxylation-decarboxylation, in agreement with the DFT results.

The different carboxylation behaviors of pyrrole and pyrazole were intriguing and suggested that, as shown for indoles above ([Scheme 6](#)), 5-membered *N*-heteroaryls can be categorized as two distinct subgroups, *stable* or *fluxional* mixed



## Scheme 7. Attempted Carboxylations of Azoles

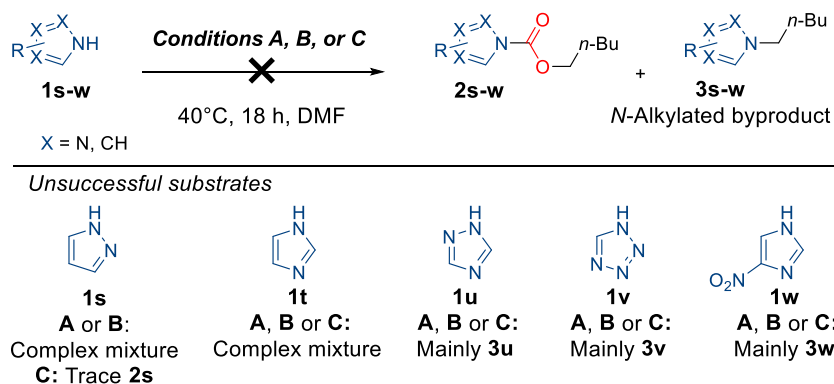


Table 2. Computed Free Energies for Mixed Carbamate Formation of 5-Membered N-Heteroaryls with TMG

$\text{TMG} + \text{HetArH} \xrightarrow{\text{CO}_2} \text{TMGH}^+ + \text{HetArCO}_2^-$

Carboxylation can occur at two types of nitrogen

**Pyridine-like nitrogen**

- Aprotic (one double bond)
- Free lone pair
- Lewis basic

**Pyrrole-like nitrogen**

- Protic (three single bonds)
- Lone pair part of the aromatic system
- Not Lewis basic

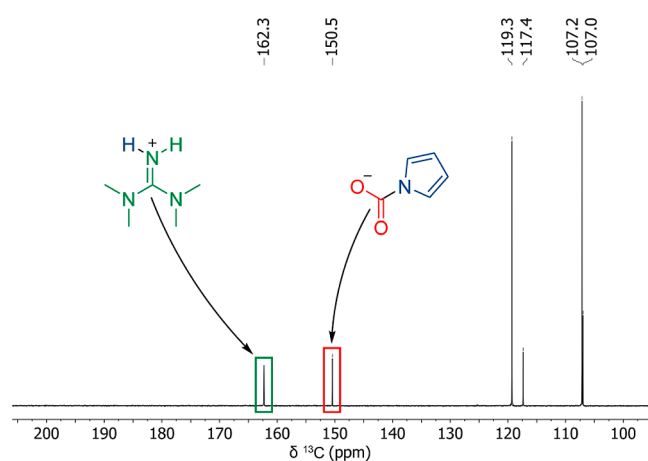
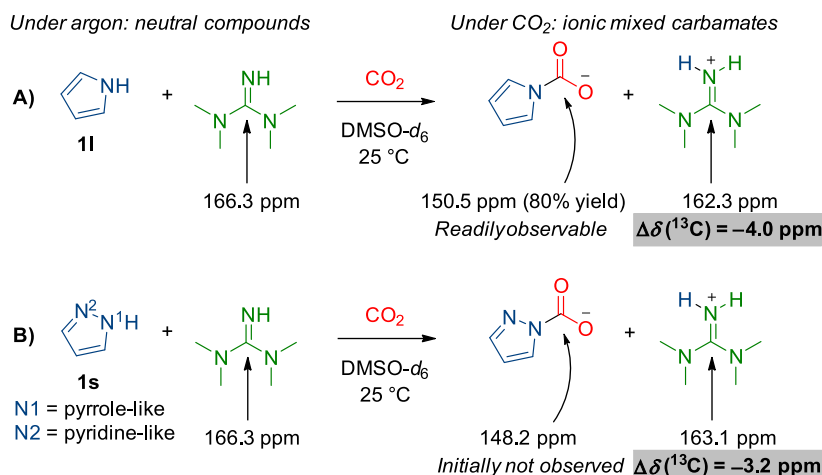
Entry	N-Heteroaryl	Reactive N	$\Delta G^\ddagger, ^a$	$\Delta G_r, ^a$
1		N1	18.2	-2.6
2		N1	17.7	-1.3
		N2	10.7	-1.3
3		N1	16.5	1.1
		N3	10.2	1.1
4		N1	14.1	0.7
		N2	11.1	0.7
		N4	8.8	3.0
5		N1	10.4	7.1
		N2	10.8	9.0
		N3	12.7	9.0
		N4	9.6	7.1
6		N1	14.5	5.6
		N3	15.0	12.3

<sup>a</sup> $\Delta G_{1M}$ , kcal/mol, 298 K, PBE0-D3BJ[IEFPCM(DMF)], see Supporting Information, Section S1 for details.

carbamates. To explore the generality of this idea, we conducted a more systematic NMR study of 5-membered N-heteroaryls (Figure 5).<sup>62</sup> Imidazole **1t** produces a very similar

<sup>13</sup>C{<sup>1</sup>H} spectrum to isomeric pyrazole **1s**. Both azoles show a broad low-intensity carboxylate, implying similar interaction with CO<sub>2</sub>. For azoles containing a third nitrogen, **1u** and isomeric 1,2,3-triazole **1u'**, the carboxylates are located somewhat more upfield than for **1s** and **1t**, retaining the low intensity, but being sharp in shape. This suggested to us that triazoles have a weaker interaction with CO<sub>2</sub>. Tetrazole **1v** contains four nitrogen atoms, and only free CO<sub>2</sub> (124.2 ppm) is detected, suggesting very little reactivity with CO<sub>2</sub> (Supporting Information, Section S15.9). Compared to imidazole **1t**, 4-nitroimidazole **1w** has a significant upfield shift of the carboxylate, suggesting that -NO<sub>2</sub> induces potent electronic destabilization. The NMR results in Figure 5 indicate that the introduction of a second, pyridine-like nitrogen into the heterocycle induces fluxional behavior. Any additional nitrogen or strongly electron-withdrawing group seems to weaken the interaction between CO<sub>2</sub> and any given azole. This observation was evaluated by measuring the CO<sub>2</sub> binding capacity of neat azole-superbase complexes using thermogravimetric analysis (TGA, Figure 5).<sup>63</sup> We found that fluxional mixed carbamates with two nitrogen atoms in the ring (**1s** and **1t**) bind ca. 0.8 equiv CO<sub>2</sub>, which is associated with a large change in protonation state ( $\Delta\delta(^{13}\text{C}) \approx -4$  ppm). This amount is approximately halved with the introduction of a third nitrogen atom (**1u** and **1u'**) or a strongly electron-withdrawing group (**1w**). A fourth nitrogen (**1v**) results in no measurable binding of CO<sub>2</sub> (for details, see Supporting Information, Section S4.3). Our findings are in line with computationally predicted CO<sub>2</sub> absorption<sup>34</sup> and previous experimental studies applying azole-superbase complexes as CO<sub>2</sub> capture materials.<sup>42,43,46</sup>

Next, the stability of azole-derived mixed carbamates under lower temperatures was investigated. First, we computed thermal effects on 1,2,4-triazole **1u** (Figure 6). The results show that the pyrrole-like nitrogen N4 has the lowest carboxylation barrier at all tested temperatures, yet its reaction energy is consistently the least favorable. In contrast, carboxylation at N2 is favorable at 248 K and even more so at 223 K, suggesting that this carbamate is the major species at low temperatures. These results are supported by VT-NMR studies (Supporting Information, Section S5.2). At 25 °C, two <sup>15</sup>N resonances are observable, assigned to pyridine-like N4 and pyrrole-like N1/N2. As the temperature is lowered, the <sup>15</sup>N signal corresponding to N4 decreases in intensity, nearly disappearing at -25 °C. This suggests that the equilibrium is shifted toward carboxylated 1,2,4-triazole **1u**, in agreement with the computed energies.

Scheme 8.  $^{13}\text{C}\{^1\text{H}\}$  NMR Experiments of Pyrrole **1l** (A) or Pyrazole **1s** (B) with TMG (1 equiv)

**Figure 3.**  $^{13}\text{C}\{^1\text{H}\}$  NMR spectrum (selected region) of pyrrole **1l** and TMG (1 equiv) under  $\text{CO}_2$  (1 bar) in  $\text{DMSO-}d_6$  at  $25^\circ\text{C}$ .

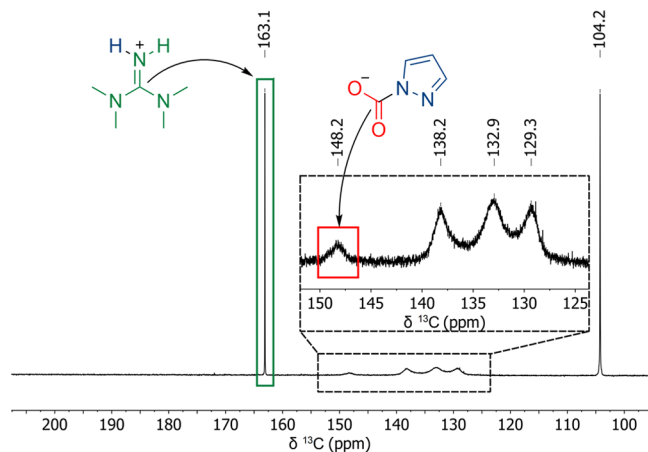


**Figure 4.**  $^{13}\text{C}\{^1\text{H}\}$  NMR spectrum (selected region) of pyrazole **1s** and TMG (1 equiv) under  $\text{CO}_2$  (1 bar) in  $\text{DMSO-}d_6$  at  $25^\circ\text{C}$ .

We then computed the reaction energies for all in situ NMR-studied *N*-heteroaryls at different temperatures (Supporting Information, Section S1.5). The results show that of the azoles **1s–1w**, pyrazole **1s** has more favorable reaction energies at lower temperatures ( $-2.9$  kcal/mol at 248 K). Indeed, VT-NMR shows that when  $\text{CO}_2$  (1 bar) is applied at

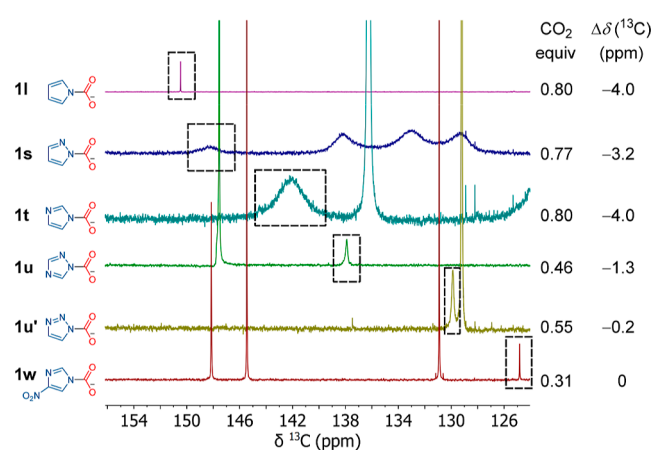


**Figure 5.** Carboxylate  $^{13}\text{C}\{^1\text{H}\}$  resonance (in dashed square) of mixed carbamates derived from 5-membered *N*-heteroaryls and TMG under  $\text{CO}_2$  (1 bar) in  $\text{DMSO-}d_6$  at  $25^\circ\text{C}$ . Note that **1l** has significantly less scans than the other experiments. Binding of  $\text{CO}_2$  equivalents at  $25^\circ\text{C}$  was determined by  $^1\text{H}$  NMR (**1l**) or TGA (**1s–1w**). See Supporting Information, Sections S4.3 and S10.

$25^\circ\text{C}$ , the  $^{15}\text{N}$  resonance of pyrazole **1s** is not detected. However, when cooled to  $-25^\circ\text{C}$ , two sharp multiplicities are detected, suggesting that the fluxional behavior of pyrazole **1s** mixed carbamate is fully stabilized, *i.e.*, the rate of  $\text{CO}_2$  exchange is slow at  $-25^\circ\text{C}$  (Supporting Information, Section S5.1). Imidazole **1t** behaves similarly but appears to be more fluxional in nature as no  $^{15}\text{N}$  signals assigned to imidazole **1t** are detectable under  $\text{CO}_2$  even at  $-25^\circ\text{C}$  (Supporting Information, Section S5.3). This is in agreement with the computational results (Supporting Information, Section S1.4). To exclude the possibility that the deuterated solvent affects the reactivity of azoles, we measured NMR of the imidazole **1t**–TMG complex under neat conditions (Supporting Information, Section S5.4). In the absence of solvent, the imidazole **1t**–TMG complex is neutral under argon, but forms an ionic salt (mixed carbamate) under  $\text{CO}_2$ . Under neat conditions, carboxylated imidazole **1t** is detectable by  $^{15}\text{N}$  NMR as a broad resonance, consistent with fast  $\text{CO}_2$  exchange and implying that the observed reactivity in solvents ( $\text{DMSO-}d_6$ ,  $\text{DMF-}d_7$ , and  $\text{CDCl}_3$ ) is extendable to neat conditions. Considering that azole-derived mixed carbamates are stabilized at low temperatures, it would be beneficial to develop

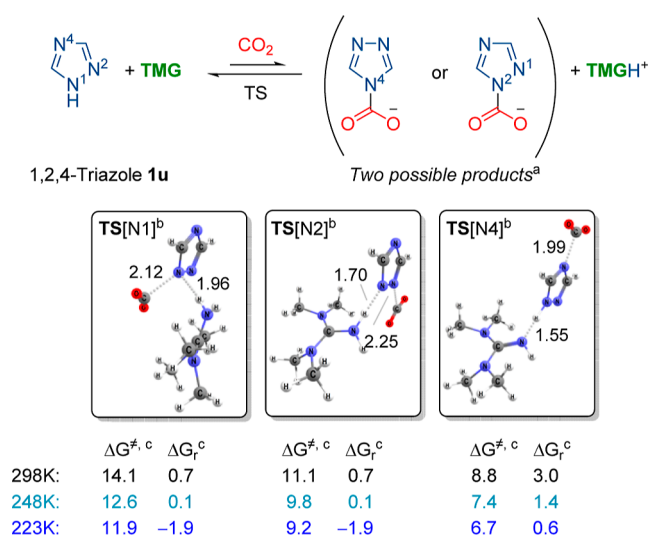


**Figure 6.** Carboxylation of 1,2,4-triazole **1u** can take place at three different nitrogens (TS[N1], TS[N2], or TS[N4]), with a preference for carboxylation at the pyridine-like nitrogens N1 and N2. <sup>a</sup>Carboxylation at N1 or N2 produces the same product. <sup>b</sup>Distances are in Angstrom. <sup>c</sup> $\Delta G_{TM}$ , kcal/mol, PBE0-D3BJ[IEFPCM(DMF)].

subsequent functionalization reactions that proceed at such low temperatures.

Finally, fused derivatives of azoles and indoles were examined in carboxylation reactions to evaluate if they behave similarly to the monocyclic counterparts (Figure 7). Indeed,

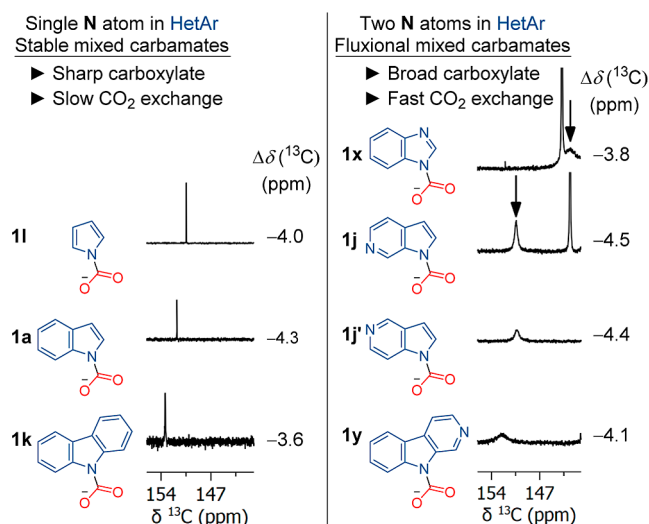
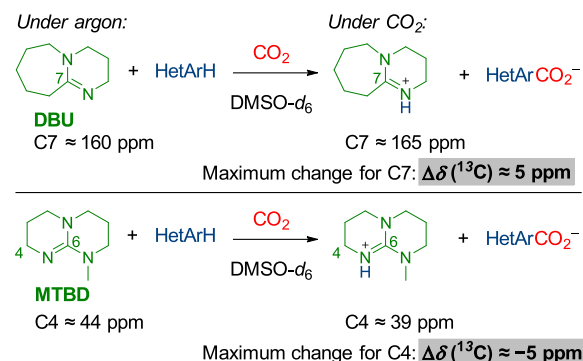


**Figure 7.** The number of nitrogen atoms in the ring structure determines whether the forming mixed carbamate will be stable or fluxional, as exemplified by the carboxylate  $^{13}\text{C}\{^1\text{H}\}$  resonance shape. TMG as the base in DMSO-*d*<sub>6</sub>, 1 bar CO<sub>2</sub>, 25 °C.

also for these substrates, more than one nitrogen in the ring system results in fluxional mixed carbamates when CO<sub>2</sub> is applied, as is seen from the broad carboxylate resonances. Large  $\Delta\delta(^{13}\text{C})$  values ( $\approx -4$  ppm) are observed, indicating that fused systems form neutral complexes with TMG, which react with CO<sub>2</sub> to form ionic salts. Consequently, the behavior of fused systems is similar to that of monocyclic *N*-heteroaryls. For details, see Supporting Information, Section S6.

**Role of Bases.** We questioned whether the observed reactivity patterns of *N*-heteroaryl–TMG complexes could be generalized to other superbases. A selection of *N*-heteroaryls was examined with DBU and MTBD, which yield largely the same carboxylation results as with TMG (Scheme 9). This

### Scheme 9. Variation of Base in *N*-Heteroaryl Carboxylations

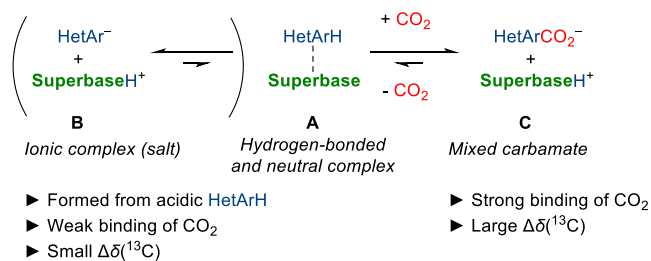


implies that *N*-heteroaryl carboxylation behavior (stable or fluxional) is minimally affected by the employed superbase. However, the CO<sub>2</sub> binding of the *N*-heteroaryl is affected by the employed superbase. With TMG (*pK*<sub>a</sub> 13.2), indole **1a** is carboxylated in 80% yield, which is increased with the stronger bases DBU (87%, *pK*<sub>a</sub> = 13.9) and MTBD (94%, *pK*<sub>a</sub> = 14.8).<sup>64</sup> We find eq 1 to be well-suited for evaluating whether DBU and MTBD form neutral complexes or ionic salts with *N*-heteroaryls. We identified DBU C7 and MTBD C4 to be sensitive toward protonation, whereas MTBD central carbon C6 is not sensitive (Supporting Information, Section S7). DBU and MTBD appear to form neutral complexes with non-acidic *N*-heteroaryls **1a** and **1t** under argon since large  $\Delta\delta(^{13}\text{C})$  values of ca. 5 ppm (DBU) or -5 ppm (MTBD) are observed (Scheme 9). In contrast, 1,2,4-triazole **1u**-based complexes have a  $\Delta\delta(^{13}\text{C})$  of 1.1 (DBU) and -0.9 (MTBD), indicating that partial deprotonation (salt formation) occurs before the introduction of CO<sub>2</sub>. The DBU or MTBD complexes with tetrazole **1v** have  $\Delta\delta(^{13}\text{C}) \approx 0$ , meaning that tetrazole **1v** is nearly fully deprotonated by both superbases under argon.

We have previously shown that aniline carboxylation yield correlates with the *pK*<sub>a</sub> of the organic base, except for sterically hindered bases.<sup>58</sup> Phosphazenes, such as tert-butylimino-tri(pyrrolidino)phosphorane (BTPP, *pK*<sub>a</sub> = 17.4), are reported to be more basic than DBU or MTBD.<sup>64</sup> Based on *pK*<sub>a</sub> alone, we expected BTPP to carboxylate indole **1a** in a high yield. However, the observed yield is only 63%. Despite BTPP being one of the least hindered phosphazenes, it seems its sterics are sufficient to partially inhibit the carboxylation of indole **1a**.<sup>65</sup>

**Mechanistic Overview.** Our overall experimental and computational results allow us to construct a comprehensive understanding of *N*-heteroaryl carbamate formation (Scheme 10). We find that under argon, superbases (TMG, DBU, and MTBD) and most *N*-heteroaryls associate by hydrogen bonding to form neutral complexes **A**. Only acidic *N*-

### Scheme 10. Reaction Pathways of *N*-Heteroaryls in the Presence of Superbases



heteroaryls (*i.e.*, tetrazole **1v** and 4-nitroimidazole **1w**) seem to exist almost completely as ionic salts **B**. Our experimental and computational results suggest a partial revision to the commonly accepted view that indoles and azoles are deprotonated by superbases, forming ionic salts.<sup>42–48</sup> Instead, most protic *N*-heteroaryls and superbases form neutral complexes (Scheme 10).

When  $\text{CO}_2$  is introduced, neutral complexes **A** are in equilibrium with mixed carbamates **C**, favoring the latter. Ionic complexes **B** have a significantly reduced affinity to  $\text{CO}_2$ , implying that they are in an unfavorable equilibrium with **C**. The number of nitrogen atoms in the ring structure and the presence of electron-withdrawing groups (EWG) determine the rate of  $\text{CO}_2$  exchange. Stable mixed carbamates exchange  $\text{CO}_2$  slowly, whereas fluxional mixed carbamates have a fast exchange. We conclude that combinations of superbases and protic *N*-heteroaryls should be considered  $\text{CO}_2$ -triggered switchable-polarity solvents (SPSs)<sup>61,66,67</sup> as they become ionic mixed carbamates first when exposed to  $\text{CO}_2$ .

## CONCLUSIONS

In summary, we report a comprehensive study on the superbase-mediated reactivity of indoles and related azoles with  $\text{CO}_2$ . We have shown that the resulting mixed carbamates can be categorized as either stable or fluxional on the basis of experimental and computational results.

The stable mixed carbamates exchange  $\text{CO}_2$  slowly and, therefore, the carbamate anion has a sufficient lifetime to readily react with alkyl bromides. The resulting *O*-alkyl carbamates are isolated in high yields (av. 86%) using mild and catalytic conditions with complete carboxylation selectivity for N1. A broad range of functional groups are tolerated, which are incompatible with conventional methods employing organometallic reagents.

Fluxional mixed carbamates undergo rapid  $\text{CO}_2$  exchange, a previously not thoroughly understood phenomenon. In this regard, we demonstrate that  $^{13}\text{C}\{^1\text{H}\}$  and  $^{15}\text{N}$  NMR are highly informative in the characterization of this compound class. Experimental and computational results suggest that fluxional behavior is caused by electronic destabilization. This is induced by two or more nitrogen atoms in the ring structure or a strongly electron-withdrawing group. These effects can be compensated by using elevated pressures of  $\text{CO}_2$  or low temperatures.

Finally, our results suggest a partial revision of the currently accepted view on how superbases react with protic *N*-heteroaryls. Under inert gas, we find that superbases and the majority of *N*-heteroaryls form neutral complexes and not ionic salts as previously thought (Scheme 10). The neutral complexes are better described as  $\text{CO}_2$ -triggered switchable-

polarity solvents as exposure to  $\text{CO}_2$  results in ionic mixed carbamates. We anticipate our work to be significant not only for  $\text{CO}_2$ -based synthesis but also in the field of  $\text{CO}_2$  capture.

## ASSOCIATED CONTENT

### Supporting Information

The Supporting Information is available free of charge at <https://pubs.acs.org/doi/10.1021/acscatal.3c02362>.

Optimized coordinates (XYZ)

Additional computational details and optimized structures, general information, general experimental procedures, reaction optimization, synthetic methods, compound characterization, details of thermogravimetric curves, HPLC results, and NMR spectra (PDF)

Crystallographic data of compound **4a-e** (CIF)

## AUTHOR INFORMATION

### Corresponding Authors

Kathrin H. Hopmann – Department of Chemistry, UiT The Arctic University of Norway, N-9037 Tromsø, Norway;

ORCID: [orcid.org/0000-0003-2798-716X](https://orcid.org/0000-0003-2798-716X);

Email: [kathrin.hopmann@uit.no](mailto:kathrin.hopmann@uit.no)

Timo Repo – Department of Chemistry, University of Helsinki, 00014 Helsinki, Finland; ORCID: [orcid.org/0000-0002-3116-6199](https://orcid.org/0000-0002-3116-6199); Email: [timo.repo@helsinki.fi](mailto:timo.repo@helsinki.fi)

### Authors

Jere K. Mannisto – Department of Chemistry, University of Helsinki, 00014 Helsinki, Finland; ORCID: [orcid.org/0000-0002-0503-2760](https://orcid.org/0000-0002-0503-2760)

Ljiljana Pavlovic – Department of Chemistry, UiT The Arctic University of Norway, N-9037 Tromsø, Norway;

ORCID: [orcid.org/0000-0002-0906-6298](https://orcid.org/0000-0002-0906-6298)

Johannes Heikkinen – Department of Chemistry, University of Helsinki, 00014 Helsinki, Finland

Tony Tiainen – Department of Chemistry, University of Helsinki, 00014 Helsinki, Finland

Aleksi Sahari – Department of Chemistry, University of Helsinki, 00014 Helsinki, Finland; ORCID: [orcid.org/0000-0002-3594-3696](https://orcid.org/0000-0002-3594-3696)

Norbert M. Maier – Department of Chemistry, University of Helsinki, 00014 Helsinki, Finland; ORCID: [orcid.org/0000-0003-3281-2604](https://orcid.org/0000-0003-3281-2604)

Kari Rissanen – Department of Chemistry, University of Jyväskylä, 40014 Jyväskylä, Finland; ORCID: [orcid.org/0000-0002-7282-8419](https://orcid.org/0000-0002-7282-8419)

Martin Nieger – Department of Chemistry, University of Helsinki, 00014 Helsinki, Finland

Complete contact information is available at: <https://pubs.acs.org/doi/10.1021/acscatal.3c02362>

### Notes

The authors declare no competing financial interest.

## ACKNOWLEDGMENTS

Dedicated to the memory of Dr. Bertel Westermarck (1948–2020), lecturer in organic chemistry. This work has been supported by NordForsk (grant no. 85378) and the members of the Nordic Consortium for  $\text{CO}_2$  Conversion (Nord $\text{CO}_2$ ), the Academy of Finland (project 310767), the Research Council of Norway (nos. 262695 and 300769), the Tromsø Research Foundation (no. TFS2016KHH), and Sigma2,



through grants of computer time (nos. nn9330k and nn4654k). J.K.M. is grateful for generous funding from the Väisälä Fund, the Orion Research Foundation, the Emil Aaltonen Foundation, the Magnus Ehrnrooth Foundation, and the Funds of Nylands Nation.

## REFERENCES

- (1) Heravi, M. M.; Zadsirjan, V. Prescribed Drugs Containing Nitrogen Heterocycles: An Overview. *RSC Adv.* **2020**, *10*, 44247–44311.
- (2) Lamberth, C. Heterocyclic Chemistry in Crop Protection. *Pest Manag. Sci.* **2013**, *69*, 1106–1114.
- (3) Vitaku, E.; Smith, D. T.; Njardarson, J. T. Analysis of the Structural Diversity, Substitution Patterns, and Frequency of Nitrogen Heterocycles among U.S. FDA Approved Pharmaceuticals. *J. Med. Chem.* **2014**, *57*, 10257–10274.
- (4) Bandini, M.; Eichholzer, A. Catalytic Functionalization of Indoles in a New Dimension. *Angew. Chem., Int. Ed.* **2009**, *48*, 9608–9644.
- (5) Xin, Z.; Lescot, C.; Friis, S. D.; Daasbjerg, K.; Skrydstrup, T. Organocatalyzed CO<sub>2</sub> Trapping Using Alkynyl Indoles. *Angew. Chem., Int. Ed.* **2015**, *54*, 6862–6866.
- (6) Felten, S.; He, C. Q.; Weisel, M.; Shevlin, M.; Emmert, M. H. Accessing Diverse Azole Carboxylic Acid Building Blocks via Mild C–H Carboxylation: Parallel, One-Pot Amide Couplings and Machine-Learning-Guided Substrate Scope Design. *J. Am. Chem. Soc.* **2022**, *144*, 23115–23126.
- (7) You, Y.; Kanna, W.; Takano, H.; Hayashi, H.; Maeda, S.; Mita, T. Electrochemical Dearomative Dicarboxylation of Heterocycles with Highly Negative Reduction Potentials. *J. Am. Chem. Soc.* **2022**, *144*, 3685–3695.
- (8) Blakemore, D. C.; Castro, L.; Churcher, I.; Rees, D. C.; Thomas, A. W.; Wilson, D. M.; Wood, A. Organic Synthesis Provides Opportunities to Transform Drug Discovery. *Nat. Chem.* **2018**, *10*, 383–394.
- (9) Dale, H. J. A.; Hodges, G. R.; Lloyd-Jones, G. C. Taming Ambident Triazole Anions: Regioselective Ion Pairing Catalyzes Direct N-Alkylation with Atypical Regioselectivity. *J. Am. Chem. Soc.* **2019**, *141*, 7181–7193.
- (10) Ghosh, A. K.; Brindisi, M. Organic Carbamates in Drug Design and Medicinal Chemistry. *J. Med. Chem.* **2015**, *58*, 2895–2940.
- (11) Schilling, W.; Das, S. Transition Metal-Free Synthesis of Carbamates Using CO<sub>2</sub> as the Carbon Source. *ChemSusChem* **2020**, *13*, 6246–6258.
- (12) Niemi, T.; Repo, T. Antibiotics from Carbon Dioxide: Sustainable Pathways to Pharmaceutically Relevant Cyclic Carbamates. *Eur. J. Org. Chem.* **2018**, 1180–1188.
- (13) Greenwald, R. B.; Zhao, H.; Xia, J.; Wu, D.; Nervi, S.; Stinson, S. F.; Majerova, E.; Bramhall, C.; Zaharevitz, D. W. Poly(Ethylene Glycol) Prodrugs of the CDK Inhibitor, Alsterpaullone (NSC 705701): Synthesis and Pharmacokinetic Studies. *Bioconjugate Chem.* **2004**, *15*, 1076–1083.
- (14) Okada, M.; Nishikibe, M. BQ-788, A Selective Endothelin ETB Receptor Antagonist. *Cardiovasc. Drug Rev.* **2006**, *20*, 53–66.
- (15) Voight, E. A.; Greszler, S. N.; Hartung, J.; Ji, J.; Klix, R. C.; Randolph, J. T.; Shelat, B. H.; Waters, J. E.; DeGoey, D. A. Desymmetrization of Pibrentasvir for Efficient Prodrug Synthesis. *Chem. Sci.* **2021**, *12*, 10076–10082.
- (16) Kim, H.; Brooks, A. D.; Dilauro, A. M.; Phillips, S. T. Poly(Carboxypyrrole)s That Depolymerize from Head to Tail in the Solid State in Response to Specific Applied Signals. *J. Am. Chem. Soc.* **2020**, *142*, 9447–9452.
- (17) Vaitla, J.; Guttormsen, Y.; Mannisto, J. K.; Nova, A.; Repo, T.; Bayer, A.; Hopmann, K. H. Enantioselective Incorporation of CO<sub>2</sub>: Status and Potential. *ACS Catal.* **2017**, *7*, 7231–7244.
- (18) Boger, D. L.; Patel, M. Activation and Coupling of Pyrrole-1-Carboxylic Acid in the Formation of Pyrrole N-Carbonyl Compounds: Pyrrole-1-Carboxylic Acid Anhydride. *J. Org. Chem.* **1987**, *52*, 2319–2323.
- (19) Boger, D. L.; Patel, M. Indole N-Carbonyl Compounds: Preparation and Coupling of Indole-1-Carboxylic Acid Anhydride. *J. Org. Chem.* **1987**, *52*, 3934–3936.
- (20) Zeng, L.; Sajiki, H.; Cui, S. Multicomponent Ugi Reaction of Indole- N-Carboxylic Acids: Expedient Access to Indole Carboxamide Amino Amides. *Org. Lett.* **2019**, *21*, 5269–5272.
- (21) Bergman, J.; Venemalm, L. Efficient Synthesis of 2-Chloro-2-Bromo- and 2-Iodoindole. *J. Org. Chem.* **1992**, *57*, 2495–2497.
- (22) Sundberg, R. J. Electrophilic Substitution Reactions of Indoles. In *Heterocyclic Scaffolds II*; Gribble, G. W., Ed.; *Topics in Heterocyclic Chemistry*; Springer Berlin Heidelberg: Berlin, Heidelberg, 2010; Vol. 26, pp 47–115.
- (23) Yoo, W. J.; Capdevila, M. G.; Du, X.; Kobayashi, S. Base-Mediated Carboxylation of Unprotected Indole Derivatives with Carbon Dioxide. *Org. Lett.* **2012**, *14*, 5326–5329.
- (24) Nemoto, K.; Onozawa, S.; Egusa, N.; Morohashi, N.; Hattori, T. Carboxylation of Indoles and Pyrroles with CO<sub>2</sub> in the Presence of Dialkylaluminum Halides. *Tetrahedron Lett.* **2009**, *50*, 4512–4514.
- (25) Yoo, W. J.; Nguyen, T. V. Q.; Guiteras Capdevila, M.; Kobayashi, S. Lithium Tert-Butoxide-Mediated Carboxylation Reactions of Unprotected Indoles and Pyrroles with Carbon Dioxide. *Heterocycles* **2015**, *90*, 1196–1204.
- (26) Xu, K.; Gilles, T.; Breit, B. Asymmetric Synthesis of N-Allylic Indoles via Regio- and Enantioselective Allylation of Aryl Hydrazines. *Nat. Commun.* **2015**, *6*, 7616.
- (27) Gnanamani, E.; Yan, X.; Zare, R. N. Chemoselective N-Alkylation of Indoles in Aqueous Microdroplets. *Angew. Chem., Int. Ed.* **2020**, *59*, 3069–3072.
- (28) Uema, S.; Saito, K.; Yamada, T. Silver-Catalyzed Carbon Dioxide Fixation on Alkynylindoles. *Org. Lett.* **2022**, *24*, 4831–4834.
- (29) Heller, S. T.; Schultz, E. E.; Sarpong, R. Chemoselective N-Acylation of Indoles and Oxazolidinones with Carbonylazoles. *Angew. Chem., Int. Ed.* **2012**, *51*, 8304–8308.
- (30) Nelson, H.; Richard, W.; Brown, H.; Medlin, A.; Light, C.; Heller, S. T. Practical Chemoselective Acylation: Organocatalytic Chemodivergent Esterification and Amidation of Amino Alcohols with N-Carbonylimidazoles. *Angew. Chem., Int. Ed.* **2021**, *60*, 22818–22825.
- (31) Jacquet, O.; Das Neves Gomes, C.; Ephritikhine, M.; Cantat, T. Recycling of Carbon and Silicon Wastes: Room Temperature Formylation of N-H Bonds Using Carbon Dioxide and Polymethylhydrosiloxane. *J. Am. Chem. Soc.* **2012**, *134*, 2934–2937.
- (32) Leong, B. X.; Teo, Y. C.; Condamines, C.; Yang, M. C.; Su, M. D.; So, C. W. A NHC-Silyliumylidene Cation for Catalytic N-formylation of Amines Using Carbon Dioxide. *ACS Catal.* **2020**, *10*, 14824–14833.
- (33) Boogaerts, I. I. F.; Fortman, G. C.; Furst, M. R. L.; Cazin, C. S. J.; Nolan, S. P. Carboxylation of N-H/C-H Bonds Using n-Heterocyclic Carbene Copper(I) Complexes. *Angew. Chem., Int. Ed.* **2010**, *49*, 8674–8677.
- (34) Firaha, D. S.; Hollöczki, O.; Kirchner, B. Computer-Aided Design of Ionic Liquids as CO<sub>2</sub> Absorbents. *Angew. Chem., Int. Ed.* **2015**, *54*, 7805–7809.
- (35) Xiong, D.; Cui, G.; Wang, J.; Wang, H.; Li, Z.; Yao, K.; Zhang, S. Reversible Hydrophobic-Hydrophilic Transition of Ionic Liquids Driven by Carbon Dioxide. *Angew. Chem., Int. Ed.* **2015**, *54*, 7265–7269.
- (36) Wang, C.; Luo, X.; Luo, H.; Jiang, D. E.; Li, H.; Dai, S. Tuning the Basicity of Ionic Liquids for Equimolar CO<sub>2</sub> Capture. *Angew. Chem., Int. Ed.* **2011**, *50*, 4918–4922.
- (37) Seo, S.; Quiroz-Guzman, M.; Desilva, M. A.; Lee, T. B.; Huang, Y.; Goodrich, B. F.; Schneider, W. F.; Brennecke, J. F. Chemically Tunable Ionic Liquids with Aprotic Heterocyclic Anion (AHA) for CO<sub>2</sub> Capture. *J. Phys. Chem. B* **2014**, *118*, 5740–5751.
- (38) Avelar Bonilla, G. M.; Morales-Collazo, O.; Brennecke, J. F. Effect of Water on CO<sub>2</sub> Capture by Aprotic Heterocyclic Anion



- (AHA) Ionic Liquids. *ACS Sustain. Chem. Eng.* **2019**, *7*, 16858–16869.
- (39) Taylor, S. F. R.; McCrellis, C.; McStay, C.; Jacquemin, J.; Hardacre, C.; Mercy, M.; Bell, R. G.; De Leeuw, N. H. CO<sub>2</sub> Capture in Wet and Dry Superbase Ionic Liquids. *J. Solution Chem.* **2015**, *44*, 511–527.
- (40) Zhang, Y.; Wu, Z.; Chen, S.; Yu, P.; Luo, Y. CO<sub>2</sub> Capture by Imidazolate-Based Ionic Liquids: Effect of Functionalized Cation and Dication. *Ind. Eng. Chem. Res.* **2013**, *52*, 6069–6075.
- (41) Jiang, B.; Huang, Z.; Zhang, L.; Sun, Y.; Yang, H.; Bi, H. Highly Efficient and Reversible CO<sub>2</sub> Capture by Imidazolate-Based Ether-Functionalized Ionic Liquids with a Capture Transforming Process. *J. Taiwan Inst. Chem. Eng.* **2016**, *69*, 85–92.
- (42) Wang, C.; Luo, H.; Jiang, D. E.; Li, H.; Dai, S. Carbon Dioxide Capture by Superbase-Derived Protic Ionic Liquids. *Angew. Chem., Int. Ed.* **2010**, *49*, 5978–5981.
- (43) Yan, H.; Zhao, L.; Bai, Y.; Li, F.; Dong, H.; Wang, H.; Zhang, X.; Zeng, S. Superbase Ionic Liquid-Based Deep Eutectic Solvents for Improving CO<sub>2</sub> Absorption. *ACS Sustain. Chem. Eng.* **2020**, *8*, 2523–2530.
- (44) Zhu, X.; Song, M.; Xu, Y. DBU-Based Protic Ionic Liquids for CO<sub>2</sub> Capture. *ACS Sustain. Chem. Eng.* **2017**, *5*, 8192–8198.
- (45) Zhu, X.; Song, M.; Ling, B.; Wang, S.; Luo, X. The Highly Efficient Absorption of CO<sub>2</sub> by a Novel DBU Based Ionic Liquid. *J. Solution Chem.* **2020**, *49*, 257–271.
- (46) Gao, F.; Wang, Z.; Ji, P.; Cheng, J. P. CO<sub>2</sub> Absorption by DBU-Based Protic Ionic Liquids: Basicity of Anion Dictates the Absorption Capacity and Mechanism. *Front. Chem.* **2019**, *6*, 1–8.
- (47) Lei, X.; Xu, Y.; Zhu, L.; Wang, X. Highly Efficient and Reversible CO<sub>2</sub> Capture through 1,1,3,3-Tetramethylguanidinium Imidazole Ionic Liquid. *RSC Adv.* **2014**, *4*, 7052–7057.
- (48) Zhang, N.; Huang, Z.; Zhang, H.; Ma, J.; Jiang, B.; Zhang, L. Highly Efficient and Reversible CO<sub>2</sub> Capture by Task-Specific Deep Eutectic Solvents. *Ind. Eng. Chem. Res.* **2019**, *58*, 13321–13329.
- (49) Zanatta, M.; Simon, N. M.; dos Santos, F. P.; Corvo, M. C.; Cabrita, E. J.; Dupont, J. Correspondence on “Preorganization and Cooperation for Highly Efficient and Reversible Capture of Low-Concentration CO<sub>2</sub> by Ionic Liquids.”. *Angew. Chem., Int. Ed.* **2019**, *58*, 382–385.
- (50) Zanatta, M.; Simon, N. M.; Dupont, J. The Nature of Carbon Dioxide in Bare Ionic Liquids. *ChemSusChem* **2020**, *13*, 3101–3109.
- (51) Wang, T.; Zhang, Y.; Huang, B.; Cai, B.; Rao, R. R.; Giordano, L.; Sun, S. G.; Shao-Horn, Y. Enhancing Oxygen Reduction Electrocatalysis by Tuning Interfacial Hydrogen Bonds. *Nat. Catal.* **2021**, *4*, 753–762.
- (52) Park, S.; Morales-Collazo, O.; Freeman, B.; Brennecke, J. F. Ionic Liquid Stabilizes Olefin Facilitated Transport Membranes Against Reduction. *Angew. Chem., Int. Ed.* **2022**, *61*, No. e202202895.
- (53) Scholten, J. D.; Leal, B. C.; Dupont, J. Transition Metal Nanoparticle Catalysis in Ionic Liquids. *ACS Catal.* **2012**, *2*, 184–200.
- (54) Puleo, T. R.; Sujansky, S. J.; Wright, S. E.; Bandar, J. S. Organic Superbases in Recent Synthetic Methodology Research. *Chem.—Eur. J.* **2021**, *27*, 4216–4229.
- (55) Smedley, C. J.; Homer, J. A.; Gialelis, T. L.; Barrow, A. S.; Koelln, R. A.; Moses, J. E. Accelerated SuFEx Click Chemistry For Modular Synthesis\*\*. *Angew. Chem., Int. Ed.* **2022**, *61*, No. e202112375.
- (56) CCDC 2282016 (4a-e) contains the supplementary crystallographic data for this paper.
- (57) Mannisto, J. K.; Sahari, A.; Lagerblom, K.; Niemi, T.; Nieger, M.; Sztanó, G.; Repo, T. One-Step Synthesis of 3,4-Disubstituted 2-Oxazolidinones by Base-Catalyzed CO<sub>2</sub> Fixation and Aza-Michael Addition. *Chem.—Eur. J.* **2019**, *25*, 10284–10289.
- (58) Mannisto, J. K.; Pavlovic, L.; Tiainen, T.; Nieger, M.; Sahari, A.; Hopmann, K. H.; Repo, T. Mechanistic Insights into Carbamate Formation from CO<sub>2</sub> and Amines: The Role of Guanidine–CO<sub>2</sub> Adducts. *Catal. Sci. Technol.* **2021**, *11*, 6877–6886.
- (59) Kim, H.; Babu, C. R.; Burgess, D. J. Quantification of Protonation in Organic Solvents Using Solution NMR Spectroscopy: Implication in Salt Formation. *Int. J. Pharm.* **2013**, *448*, 123–131.
- (60) Bordwell, F. G. Equilibrium Acidities in Dimethyl Sulfoxide Solution. *Acc. Chem. Res.* **1988**, *21*, 456–463.
- (61) Kolthoff, I. M.; Chantooni, M. K.; Bhowmik, S. Dissociation Constants of Uncharged and Monovalent Cation Acids in Dimethyl Sulfoxide. *J. Am. Chem. Soc.* **1968**, *90*, 23–28.
- (62) We note that our NMR results are in agreement with a recent study, which reported *N*-heteroaryl carboxylates as broad, low-intensity signals at ca. 150 ppm (ref 38). Other studies have reported the carboxylate as a sharp, high-intensity signal at ca 161 ppm (refs 42–48), but the accuracy of these claims have been questioned, as the signal at ca 161 ppm is proposed to be bicarbonate originating from residual moisture (refs 49 and 50). For details, see [Supporting Information](#) Section S3.2.
- (63) Van Ausdall, B. R.; Glass, J. L.; Wiggins, K. M.; Aarif, A. M.; Louie, J. A Systematic Investigation of Factors Influencing the Decarboxylation of Imidazolium Carboxylates. *J. Org. Chem.* **2009**, *74*, 7935–7942.
- (64) Tshepelevitsh, S.; Kütt, A.; Lökov, M.; Kaljurand, I.; Saame, J.; Heering, A.; Plieger, P. G.; Vianello, R.; Leito, I. On the Basicity of Organic Bases in Different Media. *Eur. J. Org. Chem.* **2019**, *2019*, 6735–6748.
- (65) Schwesinger, R. (Tert -Butylimino)Tris(Pyrrolidino)-Phosphorane (BTTP). *Encyclopedia of Reagents for Organic Synthesis*; John Wiley & Sons, Ltd: Chichester, UK, 2007; Vol. 1, pp 2–5.
- (66) Phan, L.; Andreatta, J. R.; Horvey, L. K.; Edie, C. F.; Luco, A. L.; Mirchandani, A.; Darensbourg, D. J.; Jessop, P. G. Switchable-Polarity Solvents Prepared with a Single Liquid Component. *J. Org. Chem.* **2008**, *73*, 127–132.
- (67) Pollet, P.; Davey, E. A.; Ureña-Benavides, E. E.; Eckert, C. A.; Liotta, C. L. Solvents for Sustainable Chemical Processes. *Green Chem.* **2014**, *16*, 1034–1055.